Surface Science 605 (2011) 1616–1620

Contents lists available at ScienceDirect

Surface Science

journal homepage: www.elsevier.com/ locate/susc

# Self-assembly of graphenes

Jae Hyun Park, N.R. Aluru *

*Beckman Institute for Advanced Science and Technology, Department of Mechanical Science and Engineering, University of Illinois at Urbana-Champaign, Urbana, IL 61801, United States*

ARTICLE INFO

Available online 26 February 2011

*Keywords:*
Graphene
Self-assembly
Water
Molecular dynamics simulation
Potential of mean force
Hydrogen bond

ABSTRACT

Given the technological significance of graphene, various aspects of graphene have been recently explored. Here, we demonstrate the self-assembly of graphene fragments in water using molecular dynamics simulation. We observe that graphene fragments dispersed in water are assembled into a single aggregate. The assembly process is investigated by using the potential of mean force analysis and the significance of the enthalpic and entropic contributions is described. Other fundamental quantities such as hydrogen bonding and excluded volume are also examined. We anticipate that the fundamental finding in this paper can be extended to design the assembly process of complex carbon-based structures.



## 1. Introduction

Graphene, which is defined as a single layer of graphite [1,2], has received significant attention recently because of its potential applications as chemical filters, electrical batteries, nanoelectronic and nanoelectromechanical devices, molecular storage devices, etc. [3,4]. Even though a significant amount of experimental, computational and theoretical results have been reported on graphene, many aspects of graphene are still not well understood. For example, one area where the properties of graphene haven't been understood in great detail is self-assembly. Molecular self-assembly, which is defined as the spontaneous organization of molecular units forming stable and structurally well-defined aggregates in equilibrium condition [5], has received significant attention in nanotechnology because of its potential to enable design of complex nano and biological structures [6–8]. In the present study, by performing extensive molecular dynamics simulations, we investigate the behavior of graphene fragments in water, focusing on the possibility of formation of graphite-like structure from graphene fragments through self-assembly.

## 2. Methods

The self-assembly of graphene fragments in water is investigated by performing molecular dynamics (MD) simulations. As shown in Fig. 1, initially eight small graphene fragments were uniformly distributed in water. Each fragment consists of 68 carbon atoms and its size is $1.552 \times 0.978$ nm$^2$. No hydrogen atoms are present on the terminal carbon atoms. Graphene fragments are modeled by considering all possible potentials such as stretching, bending, and torsion for bonding interactions and (6–12) Lennard–Jones (LJ) potential for non-bonding interactions [9,10]. Simulations were performed using GROMACS 4.0.4 [11] in an *NVT* ensemble. The size of the simulation box is $5 \times 5 \times 5$ nm$^3$ and periodic boundary conditions were imposed along all the three directions. The box had 3808 water molecules and the graphene fragments. The water molecules were modeled using the TIP3P model [12] and the nonbonding LJ interactions between the oxygen (OW) in water and the carbon (C) in graphene were computed using the Lorentz–Berthelot mixing rule. Electrostatic interactions were computed by using the Particle Mesh Ewald (PME) method [13]. The Nosé–Hoover thermostat [14,15] was used to maintain the system temperature at 300 K. The equation of motion was integrated by using the leapfrog algorithm with a time step of 2.0 fs. Total simulation time was 12.0 ns.

## 3. Results and discussion

The self-assembly process of graphene fragments in water is shown in Fig. 2. At t = 500 ps, the fragments formed pairs with parallel orientation — *double stacking pattern* (see Fig. 2(a)). The separation distance between the fragments in the pair was observed to be 0.354 nm, which is similar to the inter-layer distance of graphite (0.3354 nm) [16]. At t = 1800 ps, a quadruple stacking pattern appeared through the combination of two double stacking aggregates (see the upper aggregate in Fig. 2(b)). The inter-layer distance was still observed to be 0.354 nm. At t = 2400 ps, the complete assembly of all the eight fragments into a large aggregate was observed (see Fig. 2(c)) and it was stably maintained until the end of the simulation (t = 12.0 ns). The final assembled structure consists of six layered stacking and double stacking sub-structures.

The formation of double stacking pattern between two graphene fragments was further quantified in Fig. 3. The plot shows the temporal variation of the center-to-center distance and the angle between two graphenes. Initially, two graphenes are sufficiently separated (t = 120 ps). Then, they start approaching each other slowly by

* Corresponding author.
*E-mail address:* aluru@illinois.edu (N.R. Aluru).

0039-6028/$ – see front matter © 2011 Elsevier B.V. All rights reserved.
doi:10.1016/j.susc.2011.02.011

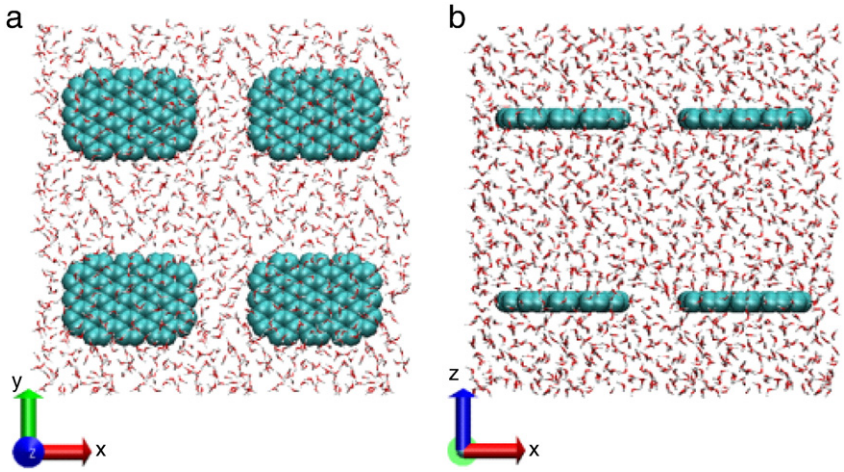


**Fig. 1.** Molecular visualization of the initial configuration of graphene fragments in water: (a) top view; (b) side view. The snapshots were rendered using VMD [28].

changing their configuration randomly (t = 140 ps). When the distance between the fragments is reduced to a certain distance (for example, at t = 174 ps, denoted as configuration A), the fragments cannot approach any further because of the geometric hindrance causing a significant energy barrier. Instead, the fragments then try to change the pairing configuration to minimize the energy of the system (t > 174 ps). As a result of continuous change in the pairing configuration (e.g. perpendicular orientation at t = 190 ps, denoted as configuration B), they eventually find the most favorable configuration — the parallel orientation where the angle between the fragments is almost zero (t = 200 ps and 220 ps, configuration C). Once the double stacking is formed, it is quite stable (t > 210 ps).

The favorable parallel pairing of graphene fragments can be explained using the PMF (potential of mean force). We considered two representative orientations (parallel versus perpendicular) for a graphene-pair (see Fig. 4). For each orientation, we performed 28 simulations by varying the distance of separation between the fragments, $r$, to compute the mean force on the fragment [17,18]. For parallel orientation, the distance of separation between the fragments was defined as the distance between the center of mass of one fragment and the center of the other fragment, while for the perpendicular orientation, it was defined as the closest distance between two fragments. In each simulation, the fragments were fixed at the distance, $r$, while water molecules were allowed to move freely. For each distance, the system was equilibrated for 4.0 ns, and the data was collected for an additional 4.0 ns of simulation time. Then, PMF, $w(r)$ as a function of separation distance, $r$, was obtained by integrating the mean force profiles, $f(r)$:

$$w(r) = -\int_{r_{ref}}^{r} f(r')dr', \tag{1}$$

where $r_{ref}$ is the reference position ($w(r_{ref}) = 0$), and is taken as the position where the mean force is zero ($r_{ref} = 1.6$ nm).

For the parallel orientation, two additional PMF profiles at $T = 285$ K and 315 K were computed to obtain the entropic contribution, $-T\Delta S(r)$, to the PMF. For a small temperature difference of $\Delta T = 15$ K, as employed in the present study, $-T\Delta S(r)$ can be approximated as [19,20]

$$-T\Delta S(r) = T\frac{w(r, T+\Delta T) - w(r, T-\Delta T)}{2\Delta T}, \tag{2}$$

which is the discretized form of the classical thermodynamic relation, $TS = -T(\partial w/\partial T)_{N,V}$. Fig. 5(a) compares the three PMF profiles at different temperatures of $T = 285$, 300, and 315 K for the graphene fragments with parallel orientation. We note that the PMF profile with higher temperature is lower compared to the profile with lower temperature. This is confirmed by computing the PMF difference, defined as PMF($T$) − PMF

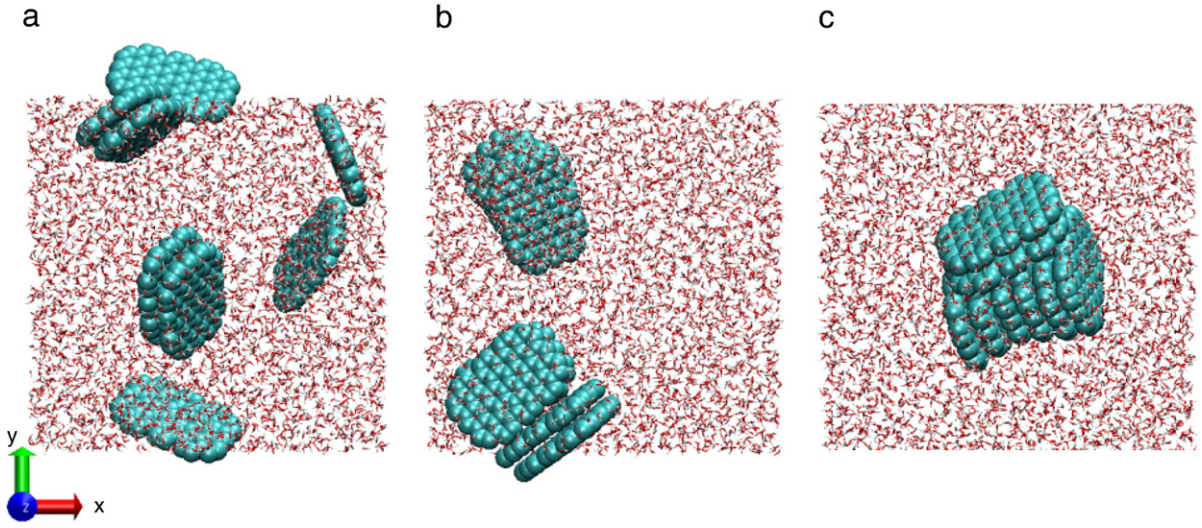


**Fig. 2.** Self-assembly of graphene fragments: (a) t = 500 ps; (b) t = 1800 ps; (c) t = 2400 ps.

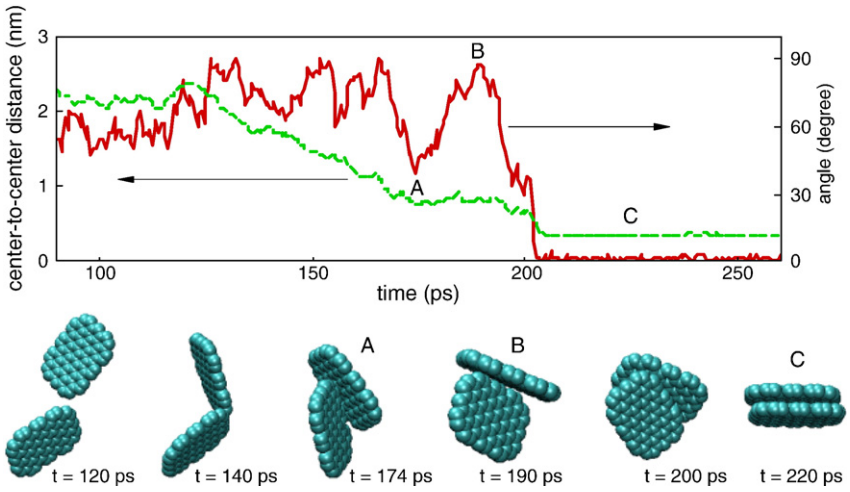


**Fig. 3.** Formation of double stacking pattern between a graphene pair.

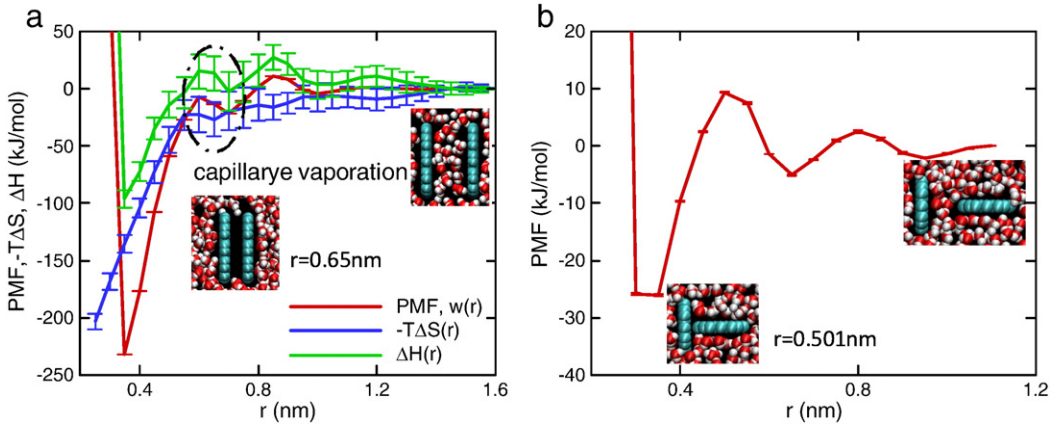


**Fig. 4.** (a) PMF, entropic contribution ($-T\Delta S$), and enthalpy ($\Delta H$) profiles for the graphene fragments with parallel orientation; (b) PMF profile for perpendicular orientation.

($T=300$ K), in Fig. 5(b). PMF($T=285$ K) − PMF($T=300$ K) is always positive while PMF($T=315$ K) − PMF($T=300$ K) is always negative.

For the parallel orientation, shown in Fig. 4(a), as we reduce the distance between the fragments, the number of waters between the graphene fragments gradually decreases and finally the *capillary evaporation* [21,22] is observed at $r=r_c=0.65$ nm (see the inset in Fig. 4(a)). For $r>r_c$, the variation of PMF is not remarkable, while, for $r<r_c$, the PMF decreases rapidly until it reaches a minimum, and then increases with a further reduction in distance. The equilibrium distance at which the minimum of PMF is observed is $r=r_{eq}=0.35$ nm and this corresponds to the average perpendicular distance between graphene fragments in stacked structures. The PMF at $r=r_{eq}$ is quite low, approximately −230 kJ/mol. For $r>r_c$, $-T\Delta S(r)$ acts as weak attraction (negative) whereas $\Delta H(r)$ acts as weak repulsion (positive). This indicates that the stacking

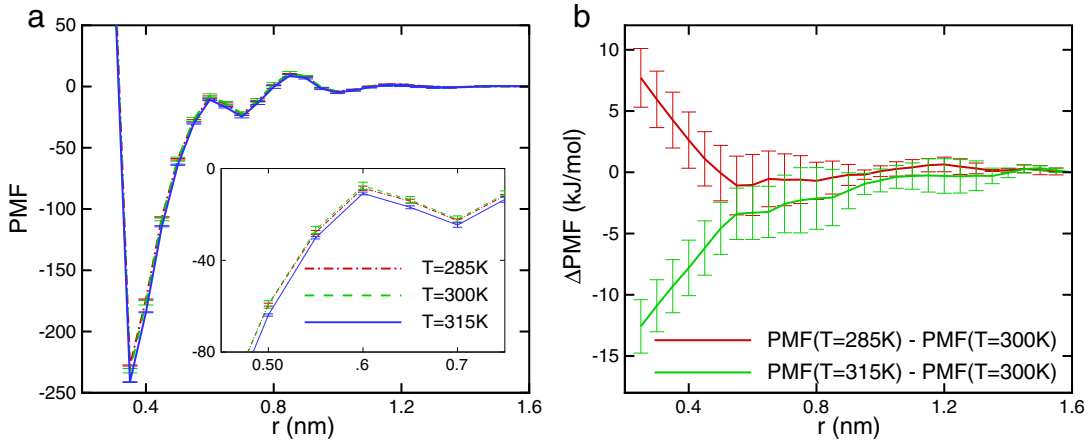


**Fig. 5.** (a) PMF profiles for $T=285$, 300, and 315 K for the graphene fragments with parallel orientation. (Inset) enlarged plot for 0.45 nm$<r<$0.75 nm; (b) PMF difference defined as $\Delta$PMF = PMF($T$) − PMF($T=300$ K) for $T=285$ and 315 K.

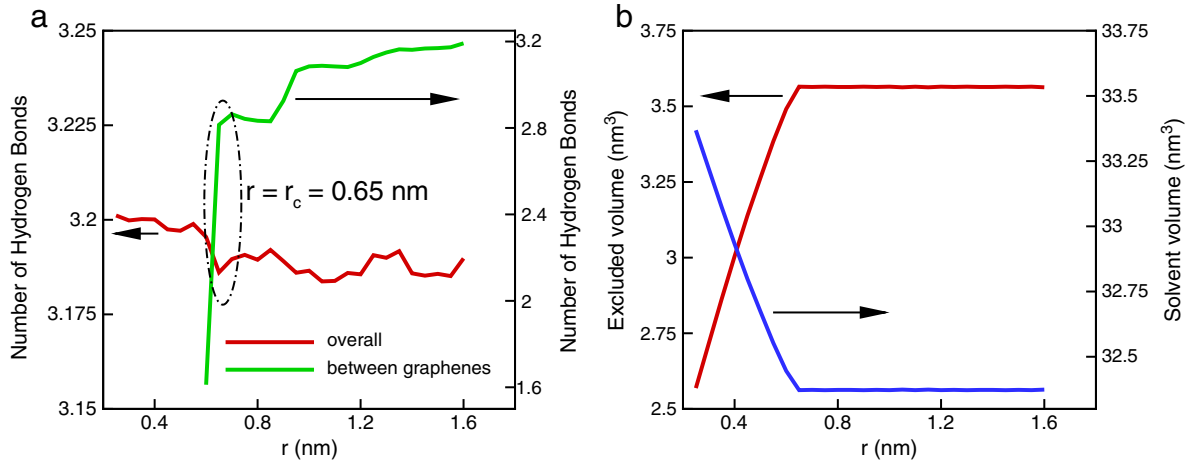


**Fig. 6.** (a) Variation of the number of hydrogen bonds (nHB) for the graphene fragments with parallel orientation. The red line denotes nHB averaged over all the water molecules while the green line denotes nHB between the two graphene fragments. $r_c$ is the position where the *capillary evaporation* happens; (b) variation of the excluded volume and solvent volume.

assembly of two graphene fragments is initiated by the entropic contribution. After the capillary evaporation ($r<r_c$), $-T\Delta S(r)$ becomes a much stronger driving force for the assembly (rapid decrease of $-T\Delta S$) [23,24]. When a graphene fragment pair is solvated in water, the water structure between the two graphene fragments is highly ordered. For $r>r_c$, with decrease in the separation distance ($r$), the amount of ordered waters in between the fragments is reduced and entropy increases. Then, when the distance reaches a critical distance ($r_c$), the gap between the fragments is so small that no water molecule can stay in. Subsequently, for $r<r_c$, entropy increases rapidly.

The above observation can be explained by considering the number of hydrogen bonds (nHB) and the excluded volume of the graphene pair [25]. In this study, the hydrogen bonds are counted by using the geometrical criterion: two water molecules are considered to be hydrogen bonded only if their oxygen–oxygen distance is less than 3.5 Å and the angle between the oxygen–oxygen axis and one of the oxygen–hydrogen bonds is less than 30° [26]. Fig. 6(a) shows the variation of nHB for graphene fragments with parallel orientation. For $r<r_c$, after capillary evaporation, the overall nHB (averaged over all the water molecules in the system) were slightly increased (see the red line in the figure), because the ordered water molecules between fragments were expelled and the amount of water molecules in the disordered state increased. The nHB between fragment clarifies such a transition (see the green line in Fig. 6(a)). Furthermore, as shown in Fig. 6(b), with decrease in the separation distance, the excluded volume of the graphene pair (the volume enclosed by the solvent accessible surface) significantly decreased along with the rapid increase in the solvent volume (defined as the excluded volume subtracted from the total volume). The increase in solvent volume leads to the increase in entropy of the solvent [27]. The enthalpic contribution, $\Delta H(r)$ also becomes attractive for $r<r_c$ due to the strong attraction between graphenes. The magnitude is, however, smaller compared to the entropic contribution. With further decrease in $r$ ($r<r_{eq}$), the enthalpic contribution becomes significantly repulsive due to the van der Waals repulsion, which makes the PMF, $w(r)$, repulsive (positive).

For the perpendicular orientation, as shown in Fig. 4(b), the capillary evaporation is not observed and the PMF at equilibrium position ($r_{eq}=0.351$ nm) is $-26$ kJ/mol. At $r_{eq}=0.351$ nm, the closest distance becomes quite similar to the size of the carbon atom in LJ (6–12) potential ($\sigma_C=0.339$ nm) and the PMF starts to abruptly increase (repulsive). For the perpendicular orientation, a significant change in water network such as capillary evaporation was not observed and the PMF cannot be lowered as in the parallel orientation. Hence, the parallel orientation is preferred for the self-assembly of graphene fragments. If the thickness of a layered graphene stacking is sufficiently large, then it can act like a graphene surface and permit the attachment of another graphene fragment. In this assembly, the new fragment has the perpendicular orientation to the graphene sheet in the multilayer sub-structure.

## 4. Conclusions

To summarize, we observe self-assembly of graphene fragments in water. The preference for parallel orientation during assembly over other orientations is explained by computing the spatial variation of the PMF for two representative orientations (parallel vs. perpendicular). For parallel orientation, the PMF significantly decreased after the capillary evaporation while for the perpendicular orientation, the capillary evaporation was not observed and the PMF between fragments is weaker compared with the parallel orientation. The main driving force in the graphene fragment assembly is the entropic contribution. The enthalpic contribution acts as an adverse factor for assembly for $r>r_c$ and for $r<r_c$, the contribution becomes favorable for assembly, however the magnitude is smaller compared to the entropic contribution. The results shown here can be used to build carbon-based complex anisotropic nanostructures [7].

## Acknowledgement

This research was supported by NSF under grant nos. 0120978, 0328 162, 0810294, 0852657, and 0915718.

## References

[1] K.S. Novoselov, A.K. Geim, S.V. Morozov, D. Jiang, Y. Zhang, S.V. Dubonos, I.V. Grigorieva, A.A. Firsov, Science 306 (2004) 666.
[2] K.S. Novoselov, D. Jiang, F. Schedin, T.J. Booth, V.V. Khotkevich, S.V. Morozov, A.K. Geim, Proc. Natl Acad. Sci. USA 102 (2005) 10451.
[3] D.A. Dikin, S. Stankovich, E.J. Zimney, R.D. Piner, G.H.B. Dommett, G. Evmenenko, S.T. Nguyen, R.S. Ruoff, Nature 448 (2007) 457.
[4] A.K. Geim, K.S. Novoselov, Nat. Mater. 6 (2007) 183.
[5] G.M. Whitesides, J.P. Mathias, C.T. Seto, Science 254 (1991) 1312.
[6] J.A.A.W. Elemans, A.E. Rowan, R.J.M. Nolte, J. Mater. Chem. 13 (2003) 2661.
[7] S.C. Glotzer, M.J. Solomon, Nat. Mater. 6 (2007) 557.
[8] G.M. Whitesides, M. Boncheva, Proc. Natl Acad. Sci. USA 99 (2002) 4769.
[9] Y. Guo, N. Karasawa, W.A. Goddard III, Nature 351 (1991) 464.
[10] N. Karasawa, S. Dasgupta, W.A. Goddard III, J. Phys. Chem. 95 (1991) 2260.
[11] D. van der Spoel, E. Lindahl, B. Hess, G. Groenhof, A.E. Mark, H.J.C. Berendsen, J. Comput. Chem. 26 (2005) 1701.
[12] W.L. Jorgensen, J. Chandrasekhar, J.D. Madura, R.W. Impey, M.L. Klein, J. Chem. Phys. 92 (1983) 926.
[13] T. Darden, D. York, L. Pedersen, J. Chem. Phys. 98 (1993) 10089.
[14] S. Nosé, Mol. Phys. 52 (1984) 255.
[15] W.G. Hoover, Phys. Rev. A 31 (1985) 1695.

[16] P. Delhaés, Polymorphism of Carbon, in: P. Delhaés (Ed.), Graphite and Precursors (World of Carbon), vol. 1, Gordon and Breach Publishers, Amsterdam, The Netherlands, 2001, p. 8, Chap. 1.
[17] C.S. Pangali, M. Rao, B.J. Berne, Mean Force of two Noble gas Atoms Dissolved in Water, in: P. Lykos (Ed.), Computer Modeling of Matter, ACS Symposium Series 86, American Chemical Society, Washington, DC, 1978, pp. 32–34.
[18] K. Watanabe, H.C. Andersen, J. Phys. Chem. 90 (1986) 795.
[19] S.W. Rick, B.J. Berne, J. Phys. Chem. B 101 (1997) 10488.
[20] D.E. Smith, A.D.J. Haymet, J. Chem. Phys. 98 (1993) 6445.
[21] N. Choudhury, B.M. Pettitt, J. Am. Chem. Soc. 127 (2005) 3556.
[22] X. Huang, R. Zhou, B.J. Berne, J. Phys. Chem. B 109 (2005) 8634.
[23] F.H. Stillinger, J. Solution Chem. 2 (1973) 141.
[24] R.M. Pashley, P.M. McGuiggan, B.W. Ninham, D.F. Evans, Science 229 (1985) 1088.
[25] T.J. Richmond, J. Mol. Biol. 178 (1984) 63.
[26] A. Luzar, D. Chandler, Nature 379 (1996) 55.
[27] H.S. Frank, M.W. Evans, J. Chem. Phys. 13 (1945) 507.
[28] W. Humphrey, A. Dalke, K. Schulten, J. Mol. Graph. 14 (1996) 33.